MONITORING OF AVALANCHES USING DAS: FROM RELEASE TO FLOW MOTION DETECTION

Cristina Pérez-Guillén*[1], Pascal Edme[2], Andri Simeon[1], Johannes Aichele[2], Alec van Herwijnen[2], Andreas Fichtner[2], Johan Gaume[1, 2]

[1]*WSL Institute for Snow and Avalanche Research SLF, Davos, Switzerland**
[2]*ETH Zurich, Zurich, Switzerland*

ABSTRACT:

The destructive power of snow avalanches and the uncertainty in predicting them demand reliable monitoring systems in mountain regions. Distributed Acoustic Sensing (DAS) provides a novel approach by transforming fibre-optic cables into dense arrays of seismic sensors with metre-scale spacing over kilometre distances. During the 2025-2026 winter season, we installed 3 km of fibre-optic cable across two avalanche release areas near Davos, Switzerland, to investigate the potential of DAS for monitoring avalanche release and flow motion. The system continuously recorded strain rate along the cable at a spatial resolution of 2 m and a sampling frequency of 1000 Hz, decreasing to 200 Hz during periods of low danger level. For avalanches releasing across the fibre, the DAS measurements captured a distinct signal associated with the initial fracture and release processes, followed by a moving signal generated by the downslope avalanche flow. To explore the continuous dataset, we converted the DAS recordings into video-like spatio-temporal representations in which avalanche signals can be distinguished from numerous natural and anthropogenic sources. During the winter, 15 avalanches were independently documented in the monitored release areas, of which 11 were detected by DAS, including events at distances of up to approximately 300 m from the fibre. These observations demonstrate the potential of DAS to monitor both avalanche release processes and subsequent flow over large areas.

KEYWORDS: Avalanche Detection, Distributed Acoustic Sensing (DAS) Monitoring, Avalanche Release

1. INTRODUCTION

The destructive power of snow avalanches and the uncertainty in predicting them demand reliable early-detection systems in mountain regions. Standard automatic snow avalanche detection systems consist of radars, seismo-acoustic sensors or a combination. Whereas radars operate almost independently of weather conditions and are highly reliable (Köhler et al. 2018; Meier et al. 2016), their detection range is usually limited to a single slope. In contrast, seismo-acoustic monitoring systems can detect avalanches across multiple avalanche paths within a radius of several kilometres (Suriñach et al. 2000; Hammer et al. 2017; Pérez-Guillén et al. 2019; Mayer et al. 2022; Seupel et al. 2026). Despite these advances, existing detection systems remain insufficient to cover large avalanche-prone areas.

Distributed Acoustic Sensing (DAS) has emerged as a novel technology in seismic data acquisition, providing substantially higher spatial coverage than traditional monitoring systems (Walter et al. 2020). DAS systems transform standard telecommunication optical fibres into a very large number of ground deformation sensors with a metre-scale measurement point spacing (Lindsey and Martin 2021). These systems consist of an Interrogation Unit (IU) that emits and receives laser pulses in a fibre-optic cable. Hence, a single instrument forms a high-resolution distributed sensing antenna potentially over several tens of kilometres, making large-scale real-time monitoring logistically feasible and cost-effective. Therefore, these systems open new opportunities for monitoring various cryospheric processes (Walter et al. 2020; Fichtner et al. 2025) and, in particular, snow avalanches.

Prokop et al. (2014) deployed a DAS system for avalanche monitoring for the first time at an Austrian ski resort, recording 60 natural and artificially triggered avalanches with runouts of up to ≈ 250 m and assessing whether they reached critical infrastructure. Paitz et al. (2022) demonstrated the potential of DAS for avalanche monitoring using an existing telecommunication fibre-optic cable at the Vallée de la Sionne avalanche test site in Switzerland. By applying a Bayesian Gaussian Mixture Model, they automatically detected avalanches in the DAS recordings, distinguished between avalanche-generated near- and far-field seismic signals, and characterised the avalanche

* *Corresponding author address:*
Cristina Pérez-Guillén
WSL Institute for Snow and Avalanche Research SLF
Flüelastrasse 11, 7260 Davos Dorf
email: cristina.perez@slf.ch

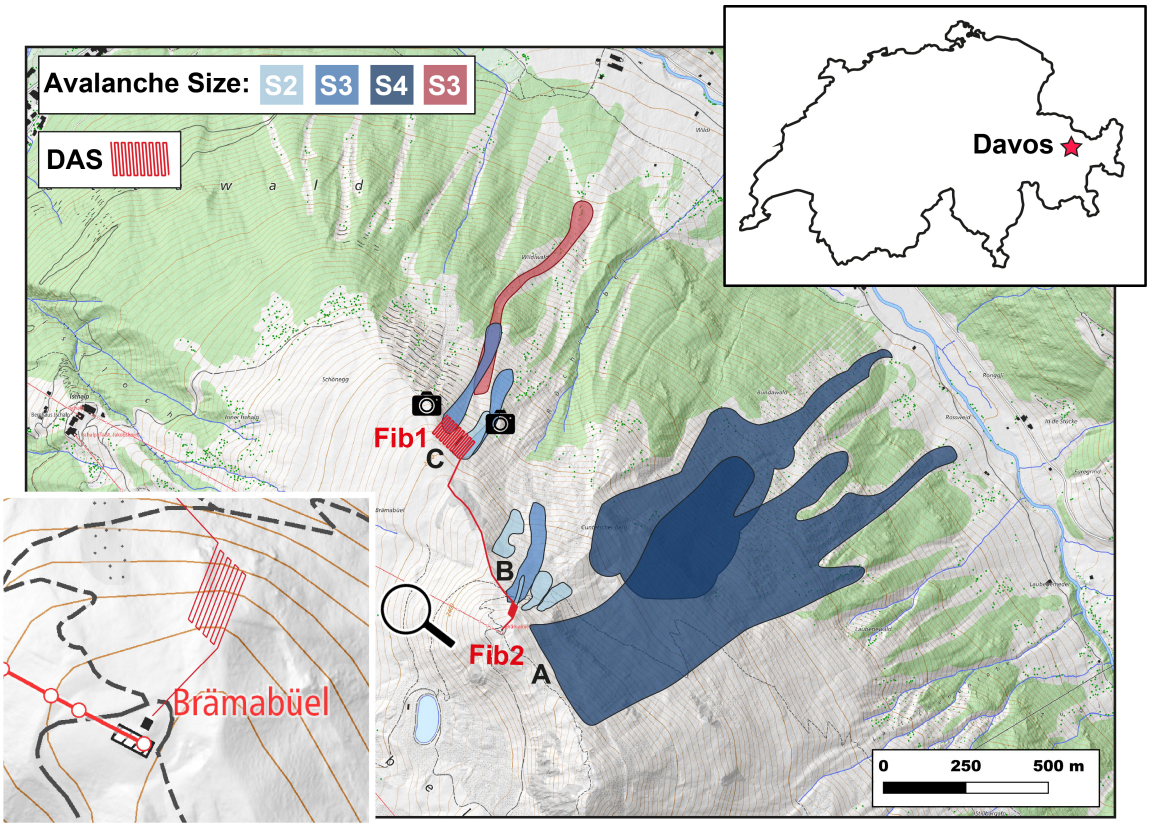


Figure 1: Overview of the study area showing the location of Brämabüel in the Davos region, Switzerland, and the layout of the Distributed Acoustic Sensing (DAS) system covering two avalanche release areas on the north- and northeast-facing slopes of Brämabüel: Fib1 in release area C and Fib2 in release area B (zoomed map of the upper Brämabüel area). The map also shows the outlines of the avalanches released during the 2025–2026 winter season, classified by avalanche type (blue: dry-snow avalanches; red: wet-snow avalanches) and size, ranging from size 2 (S2) to size 4 (S4). Map source: Swiss Federal Office of Topography.

flow. Recently, Turquet et al. (2024) installed a DAS system along an avalanche-prone road near Tromsø (Norway), detecting all eight avalanches that reached the road while simultaneously tracking vehicle location and speed. Finally, Edme et al. (2026) further demonstrated the capability of DAS for near real-time avalanche monitoring by interrogating a 10 km telecommunication fibre-optic cable along the Flüelapass road near Davos, Switzerland. Using a dual-frequency short-term/long-term average detector, they successfully discriminated avalanche signals from traffic noise and detected 91 visually confirmed avalanches over 131 monitoring days, demonstrating that existing telecommunication fibre-optic infrastructure can provide a promising solution for operational avalanche monitoring.

To further explore the capabilities of a DAS system for early avalanche detection, in this study, we installed a 3-km-long fibre-optic cable covering two avalanche release areas in Davos (Switzerland; Figure 1) during the 2025–2026 winter season. The DAS system captured the flow motion of multiple avalanches and recorded the initial fracture processes, enabling detection of the avalanche release processes. Avalanches detected in the continuous DAS recordings were validated using time-synchronised camera observations, field observations, and regular snowpack profiles, providing a comprehensive record of avalanche activity throughout the study period.

2. TEST SITE

The study site is located at the top of Brämabüel, near the Jakobshorn ski resort in Davos, Switzerland. The avalanche release areas extend from approximately 2200 to 2500 m a.s.l., on north- to northeast-facing slopes with inclinations ranging from 30° to 45° (Figure 1). Avalanches release frequently and can reach large dimensions, with runout distances extending to the road at the bottom of the Dischma Valley, where they have

Table 1: Summary of the avalanche events detected during the 2025–2026 winter season. Event: event number; Datetime (UTC): date and time of avalanche release; Release location: A, B or C (Figure 1); DAS detection: Fib1, Fib2 or No (if neither fibre detected the avalanche); DAS over: Yes if the avalanche flowed directly over the fibre, No otherwise; Aval trigger (triggering mechanism): Person, Natural, Explosive, or – if unknown; Aval size (avalanche size): S2, S3 or S4, following the European avalanche size scale EAWS21sizeScale; Aval type (avalanche type): dry- or wet-snow avalanche.

Event	Datetime (UTC)	Release location	DAS detection	DAS over	Aval trigger	Aval size	Aval type
Av 1	2026-01-11T11:16	B	Fib2	Yes	Person	S2	Dry
Av 2	2026-01-11T11:00	B	No	No	Person	S2	Dry
Av 3	2026-01-11T11:00	B	No	No	–	S2	Dry
Av 4	2026-01-11T11:00	B	No	No	Person	S2	Dry
Av 5	2026-01-21T10:33	C	Fib1	Yes	Person	S2	Dry
Av 6	2026-02-15T14:15	A	No	No	Person	S4	Dry
Av 7	2026-02-16T23:37	C	Fib1	Yes	Natural	–	Dry
Av 8	2026-02-17T17:14	C	Fib1	Yes	Natural	–	Dry
Av 9	2026-02-18T10:00	B	Fib2	No	Person	S3	Dry
Av 10	2026-02-18T10:00	B	Fib2	No	Person	S3	Dry
Av 11	2026-02-20T10:25	B	Fib2	No	Person	S3	Dry
Av 12	2026-02-22T07:54	C	Fib1	Yes	Explosive	S3	Dry
Av 13	2026-02-22T07:55	B	Fib2	No	Explosive	S3	Dry
Av 14	2026-02-22T07:55	A	Fib2	No	Explosive	S3	Dry
Av 15	2026-04-13T14:30	C	Fib1	No	Natural	S3	Wet

caused damage to both the road and the surrounding forest in the past (Glaus et al. 2025). Figure 1 provides an overview of the study site together with the mapped outlines of the avalanches released during the winter season 2025-2026. In addition, a monitoring system consisting of two low-cost lidar and optical sensors has continuously measured high-resolution variations in snow depth (Ruttner et al. 2025) in the avalanche release area denoted as C in Figure 1. The two measurement stations are co-located with automatic cameras that acquire hourly images of the slope. In addition, a third webcam installed on the opposite slope provides continuous monitoring of the entire north-facing Brämabüel avalanche paths.

Several automatic weather stations (AWS) belonging to the Intercantonal Measurement and Information System (IMIS) network (IMIS station network) are installed in Davos in high-alpine terrain. Using these meteorological observations as input, the snow-cover model SNOWPACK (Lehning et al. 1999; Morin et al. 2020) simulates snow stratigraphy. In addition, manual snow profiles were recorded in the study area approximately every two weeks to provide detailed observations of the snow stratigraphy. These data were collected for operational avalanche forecasting and are used in this study to characterise the snowpack conditions at the time and location of the detected avalanche releases.

2.1. DAS system

We installed a total of 3 km of fibre-optic cable covering two avalanche release areas (B and C in Figure 1). The two fibre-optic cables were deployed along parallel transects aligned with the main slope direction: the main fibre (Fib 1 in Figure 1), located at approximately 2250 m a.s.l., and a second fibre (Fib 2 in Figure 1), installed near the top of Brämabüel at approximately 2470 m a.s.l. The cables were anchored directly to the ground before the first snowfall in October and were subsequently buried by the seasonal snowpack. The interrogation unit (IU) was installed at the upper station of the Bräma chairlift. The DAS interrogator continuously monitored both fibres with a spatial resolution of 2 m and a sampling frequency of 1000 Hz, which was decreased to 200 Hz during periods of low avalanche danger. The DAS system operated continuously from mid-December until the end of April.

3. RESULTS

During the last winter season, a total of 15 avalanches were triggered in the three main release areas on the northern slopes of Brämabüel (Figure 1). Table 1 summarises all events, classified according to their triggering mechanism (per-

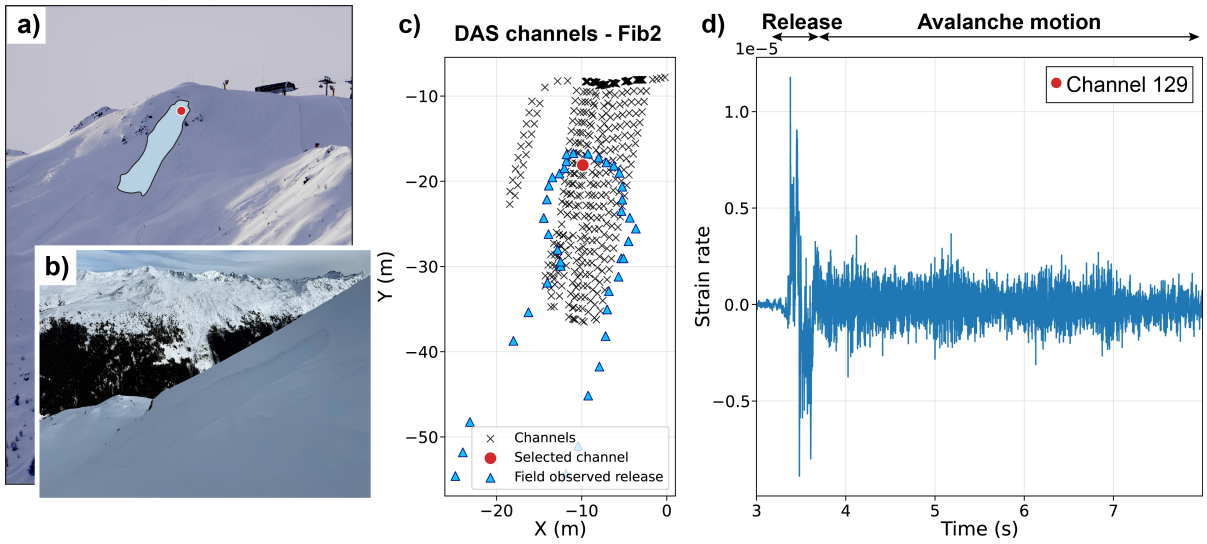


Figure 2: (a) Photograph of the top of the northern Brämabüel slope showing the outline of the skier-triggered avalanche released on 11 January 2026 (Av 1 in Table 1). (b) Photograph of the avalanche deposits. (c) 2D map of the DAS channels along Fib2 (black crosses) installed in the release area (Figure 1), and the outline of the avalanche deposit obtained from GPS measurements (blue dots). The red dot indicates the DAS channel selected for plotting the strain-rate signal shown in (d). The first part of the signal captures the avalanche release, i.e. the fracture processes, followed by the subsequent avalanche motion.

son, explosive, or natural), avalanche size, ranging from size 2 (medium) to size 4 (very large), and snow conditions (dry or wet).

3.1. DAS detections

Avalanche signals are mixed with numerous other sources detected by the DAS system, including skiers, ski lift operations, snow-grooming machines, helicopters, earthquakes, and other unknown sources, making this a real-world monitoring experiment. All avalanche events were first visually identified in the videos and subsequently verified using images from the cameras and laser scanners or through field observations. An example of the first avalanche release on 11 January 2026 and the corresponding strain-rate signal from one of the Fib2 channels are shown in Figure 2. The first part of the signal is generated by fracture processes during avalanche release in the snowpack ($t < 4$ s), which started near the selected channel (red dot in Figure 2b), while the subsequent avalanche motion generated deformation along the cable. Similar signals were recorded in the other channels, allowing the application of beamforming methods to localise the sources.

3.2. Continous monitoring

To reduce the large volume of spatio-temporal DAS data recorded continuously and facilitate the identification of potential avalanche events, we converted the continuous signals into video-like representations. Three examples of dry-snow avalanches triggered by a skier, naturally during a snowstorm, and artificially using explosives are shown in Figure 3. The colours represent the amplitudes of the Power Spectral Density (PSD; RGB representation) as a function of time (y-axis) and DAS channel (x-axis), with the latter corresponding to the distance in metres along the fibre-optic cable from the interrogator. The red box in each video frame highlights the spatio-temporal signal associated with the avalanche. Avalanche signals are characterised by a coincident onset across multiple channels, followed by a moving signal corresponding to the downslope avalanche motion. The amplitude of the strain signal appears to propagate symmetrically in opposite directions across some channels, reflecting the deployment of the fibre-optic cable in parallel up- and downslope transects aligned with the main avalanche flow direction (Figure 1).

Other signal sources can also be identified in the selected video frames. For Av 5 (Figure 3b), the signals associated with the skiers are visible as they approach the release area, passing close to the cable, and later while taking measurements in the snowfield. Av 7 (Figure 3d) shows a band of nearly constant amplitude over the first section of the fibre (200–300 m), produced by the

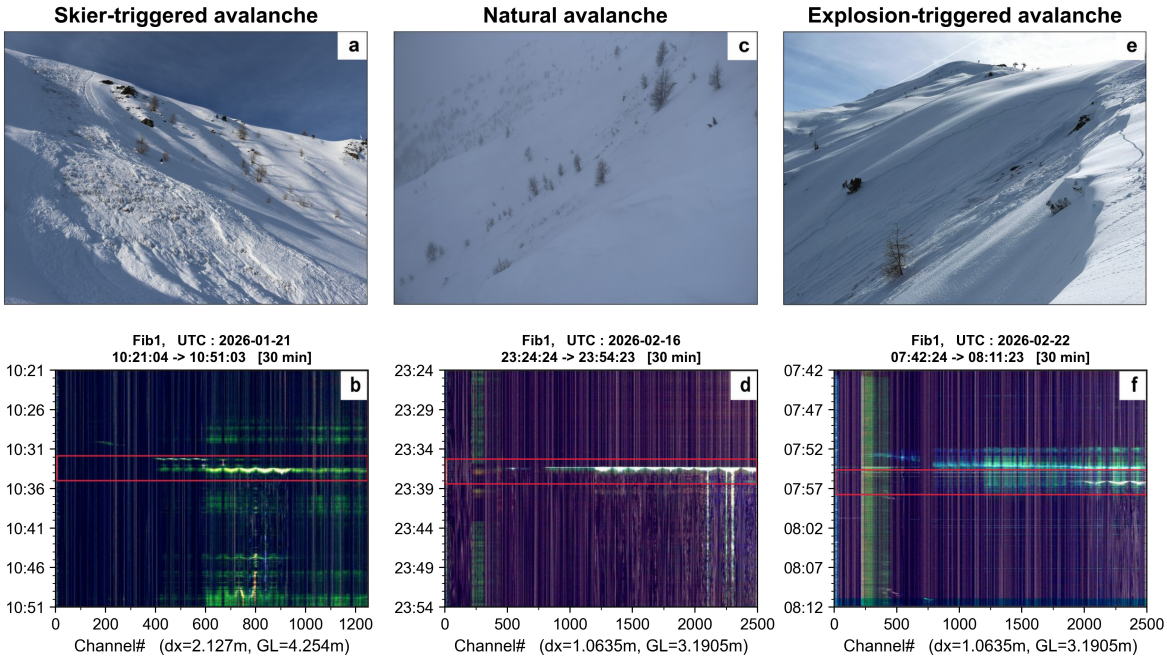


Figure 3: a) Photograph of the deposits of a skier-triggered avalanche released over Fibre 1 on 21 January 2026 at 10:33 UTC (Av 5 in Table 1), and (b) the corresponding DAS video frame showing the avalanche signal (red box). (c) Photograph of the deposits of a natural avalanche released over Fibre 1 on 16 February 2026 at 23:37 UTC (Av 7 in Table 1), and (d) the corresponding DAS video frame showing the avalanche signal (red box). (e) Photograph of the deposits of an explosion-triggered avalanche released over Fibre 1 on 22 February 2026 at 07:57 UTC (Av 12 in Table 1), and (f) the corresponding DAS video frame showing the avalanche signal (red box).

snow-grooming machine operating on the ski slope of Bramäbüel at night. A similar band is visible for Av 12 (Figure 3f) approximately at channels 200–400 m, in this case produced by the ski lift operation. In addition, the helicopter produces high-amplitude background noise, particularly before the avalanche release, as it approaches the slope to deploy the explosive charge onto the snow. The explosions produce high-amplitude, short-duration signals, visible as horizontal lines in the DAS recordings. Several explosions triggered multiple avalanches that day, when the Davos SOS team carried out avalanche control operations to secure the ski slopes and infrastructure due to the high avalanche danger.

3.3. Snowpack and avalanche activity

The winter season was characterised by a highly unstable snowpack, as shown by the seasonal snowpack simulation in Figure 4 for the AWS of the Weissflujoch snow test site of SLF, which is located at 2536 m a.s.l. at a distance of approximately 8 km from the avalanche release areas. The simulated snowpack structure was consistent with manual snow profiles collected by different SLF observers throughout the season. The snowpack was characterised by a weak base consisting of large depth hoar crystals (dark blue in Figure 4) that acted as a weak layer for avalanche release throughout the season, especially after snowfall events in mid-January and mid February. In contrast, only one wet-snow avalanche was observed at the end of the season, in early April, when the uppermost snow cover layer had transformed into a typical wet-snow layer consisting of melt forms.

3.4. Detection range

From the total of the 15 avalanches releases during the winter season (Table 1), 11 were detected by the DAS system: four flowed directly over Fib1 and only one over Fib2, while the remaining six were detected within a maximum detection range of approximately 300 m. This detection range is low compared with that reported in previous studies (Edme et al. 2026; Paitz et al. 2022). This difference may be related to the installation configuration and, in particular, to the coupling between the fibre-optic cable and the ground. In this study, the cables were installed directly on the ground surface and subsequently covered by snow, potentially resulting in weaker ground coupling compared with installations in which the fibre-optic ca-

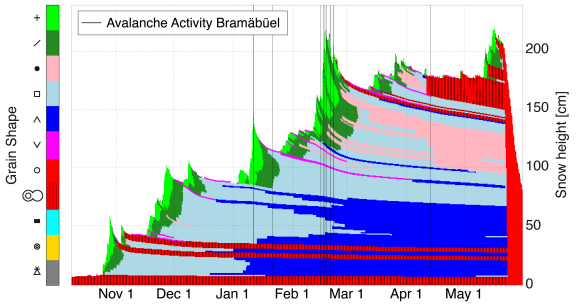


Figure 4: SNOWPACK simulation driven by data from the automatic weather station at Weissfluhjoch (2536 m a.s.l.), located approximately 8 km from the typical avalanche release areas of Brämabüel. The simulation shows the seasonal evolution of the snow stratigraphy (colors and grain-type labels follow the International Classification for Seasonal Snow on the Ground; Fierz et al. (2009)), with the vertical axis representing snow height over time. Black lines show the timing of avalanche releases during the 2025–2026 winter season.

ble is buried in the ground within a duct. In addition, the low cohesion of the base and overlying snowpack layers may have reduced the transmission of avalanche-generated seismic waves through the snowpack and into the ground, thereby limiting their detection.

4. CONCLUSIONS

We deployed a 3 km fibre-optic cable directly across two frequently active avalanche release areas at Brämabüel (Davos, Switzerland) and operated it continuously from mid-December to the end of April of the 2025–2026 winter season. In contrast to previous DAS avalanche studies, which interrogated existing telecommunication infrastructure, the cable was installed within the steep slopes of avalanche starting zones, allowing the release process to be observed in situ.

Of the 15 avalanches documented in the three main release areas, 11 were detected by the DAS system. Five events flowed directly over one of the two fibres, while the remaining six were recorded at distances of up to approximately 300 m. For slab avalanches flowing over the cable, the strain-rate signals two distinct phases: an initial signal associated with fracture processes, followed by a coherent moving signal tracking the downslope motion of the flow. DAS therefore provides not only an accurate release time, as conventional seismic systems do, but also a spatio-temporal record of the avalanche fracture processes and motion.

The maximum detection range obtained here is considerably shorter than that reported in earlier deployments. We attribute this primarily to the coupling conditions: the cables were anchored at the ground surface and subsequently buried by snow, rather than embedded in a duct. In addition, the very weak, low-cohesion basal layers that characterised the winter season likely attenuated the transmission of avalanche-generated seismic energy into the ground. The same snowpack structure, however, favoured avalanche activity during the winter season.

Converting the continuous recordings into video-like representations proved effective for reducing the high-dimensional DAS data volume and for visually identifying candidate events among the many anthropogenic and natural sources present at an operating ski area. In the future, combined with machine-learning-based feature extraction and clustering, this framework could allow avalanche signals to be automatically distinguished from other signal sources. Next steps will focus on developing automated detection models, quantifying their performance across multiple seasons and optimising cable installation to extend the effective detection range. Additionally, since the system records precursory signals associated with the fracture processes prior to avalanche release, developing detection models specifically trained to identify these signals could enable earlier detection than conventional monitoring systems, which are triggered when the avalanche is already in motion.

ACKNOWLEDGEMENTS

This work was supported by the Swiss National Science Foundation (SNSF) under SNSF Grant 10001041. We would especially like to thank the landowners for allowing the installation of the fibre-optic cables, as well as all the staff and the SOS team of the Jakobshorn ski area for allowing us to use their infrastructure and for their invaluable support during the fieldwork and the winter season. We also thank all the researchers and students from SLF and ETH Zurich who contributed to the fieldwork.

REFERENCES

Edme, P., Pérez-Guillén, C., Herwijnen, A. van, Aichele, J., Simeon, A., Paitz, P., Walter, F., and Fichtner, A. (2026). Method for near real-time detection of snow avalanches using Distributed Acoustic Sensing. In: Nat-

ural Hazards and Earth System Sciences 2026, pp. 1–33. https://doi.org/10.5194/egusphere-2026-2373.

Fichtner, A., Hofstede, C., Kennett, B. L., Svensson, A., Westhoff, J., Walter, F., Ampuero, J.-P., Cook, E., Zigone, D., Jansen, D., et al. (2025). Hidden cascades of seismic ice stream deformation. In: Science 387.6736, pp. 858–864. https://doi.org/10.1126/science.adp8094.

Fierz, C., Armstrong, R. L., Durand, Y., Etchevers, P., Greene, E., McClung, D. M., Nishimura, K., Satyawali, P. K., and Sokratov, S. A. (2009). The international classification for seasonal snow on the ground. In.

Glaus, J., Wikstrom Jones, K., Bartelt, P., Christen, M., Stoffel, L., Gaume, J., and Bühler, Y. (2025). Simulation of cold-powder snow avalanches considering daily snowpack and weather situations. In: Natural Hazards and Earth System Sciences 25.7, pp. 2399–2419. https://doi.org/10.5194/nhess-25-2399-2025.

Hammer, C., Fäh, D., and Ohrnberger, M. (2017). Automatic detection of wet-snow avalanche seismic signals. In: Nat Hazards 86, pp. 601–618. https://doi.org/10.1007/s11069-016-2707-0.

Köhler, A., McElwaine, J. N., and Sovilla, B. (2018). GEODAR Data and the Flow Regimes of Snow Avalanches. In: Journal of Geophysical Research: Earth Surface 123.6, pp. 1272–1294. ISSN: 2169-9011. https://doi.org/10.1002/2017JF004375.

Lehning, M., Bartelt, P., Brown, B., Russi, T., Stöckli, U., and Zimmerli, M. (1999). SNOWPACK model calculations for avalanche warning based upon a new network of weather and snow stations. In: Cold Regions Science and Technology 30.1-3, pp. 145–157. https://doi.org/10.1016/S0165-232X(99)00022-1.

Lindsey, N. J. and Martin, E. R. (2021). Fiber-optic seismology. In: Annual Review of Earth and Planetary Sciences 49, pp. 309–336. https://doi.org/10.1146/annurev-earth-072420-065213.

Mayer, S., Herwijnen, A. van, Techel, F., and Schweizer, J. (2022). A random forest model to assess snow instability from simulated snow stratigraphy. In: The Cryosphere 16.11, pp. 4593–4615. https://doi.org/10.5194/tc-2022-34.

Meier, L., Jacquemart, M., Blattmann, B., and Arnold, B. (2016). "Real-Time Avalanche Detection with Long-Range, Wide-Angle Radars for Road Safety in Zermatt, Switzerland". In: Proc. International Snow Science Workshop, pp. 304–308.

Morin, S., Horton, S., Techel, F., Bavay, M., Coléou, C., Fierz, C., Gobiet, A., Hagenmuller, P., Lafaysse, M., Ližar, M., et al. (2020). Application of physical snowpack models in support of operational avalanche hazard forecasting: A status report on current implementations and prospects for the future. In: Cold Reg. Sci. Technol. 170, p. 102910. https://doi.org/10.1016/j.coldregions.2019.102910.

Paitz, P., Lindner, N., Edme, P., Huguenin, P., Hohl, M., Sovilla, B., Walter, F., and Fichtner, A. (2022). Phenomenology of Avalanche Recordings from Distributed Acoustic Sensing. In: ESSOAr. https://doi.org/10.1002/essoar.10512949.1.

Pérez-Guillén, C., Tsunematsu, K., Nishimura, K., and Issler, D. (2019). Seismic location and tracking of snow avalanches and slush flows on Mt. Fuji, Japan. In: Earth Surface Dynamics 7.4, pp. 989–1007.

Prokop, A., Schön, P., Wirbel, A., and Jungmayr, M. (2014). "Monitoring avalanche activity using distributed acoustic fiber optic sensing". In: Proceedings of the international snow science workshop, pp. 129–133.

Ruttner, P., Voordendag, A., Hartmann, T., Glaus, J., Wieser, A., and Bühler, Y. (2025). Monitoring snow depth variations in an avalanche release area using low-cost lidar and optical sensors. In: Natural Hazards and Earth System Sciences 25.4, pp. 1315–1330. https://doi.org/10.5194/nhess-25-1315-2025.

Seupel, C., Pérez-Guillén, C., Fichtner, A., and Herwijnen, A. van (2026). Seismo-acoustic characterization and array processing of dry-and wet-snow avalanches. In: Journal of Geophysical Research: Earth Surface 131.7, e2025JF008947. https://doi.org/https://doi.org/10.1029/2025JF008947.

Suriñach, E., Sabot, F., Furdada, G., Vilaplana, J., et al. (2000). Study of seismic signals of artificially released snow avalanches for monitoring purposes. In: Physics and Chemistry of the Earth, Part B: Hydrology, Oceans and Atmosphere 25.9, pp. 721–727.

Turquet, A., Wuestefeld, A., and Finn Kåre Nyhammer, E. N. (2024). Advances in Avalanche Monitoring in Norway: Insights from Distributed Acoustic Sensing. In: EGU General Assembly 2024. https://doi.org/10.5194/egusphere-egu24-7603.

Walter, F., Gräff, D., Lindner, F., Paitz, P., Köpfli, M., Chmiel, M., and Fichtner, A. (2020). Distributed acoustic sensing of microseismic sources and wave propagation in glaciated terrain. In: Nature communications 11.1, p. 2436. https://doi.org/10.1038/s41467-020-15824-6.